DOI: 10.1002/cphc.200900270

110 Years of the Meyer–Overton Rule: Predicting Membrane Permeability of Gases and Other Small Compounds

Andreas Missner and Peter Pohl*[a]

The transport of gaseous compounds across biological membranes is essential in all forms of life. Although it was generally accepted that gases freely penetrate the lipid matrix of biological membranes, a number of studies challenged this doctrine as they found biological membranes to have extremely low gas-permeability values. These observations led to the identification of several membrane-embedded "gas" channels, which facilitate the transport of biological active gases, such as carbon dioxide, nitric oxide, and ammonia. However, some of these findings are in contrast to the well-established solubility–diffusion model (also known as the Meyer–Overton rule), which predicts membrane permeabilities from the molecule's oil–water partition coefficient. Herein, we discuss recently reported violations of the Meyer–Overton rule for small molecules, including carboxylic acids and gases, and show that Meyer and Overton continue to rule.

1. Introduction

110 years ago, Meyer and Overton established a simple rule to predict membrane permeabilities.[1,2] This rule does not account for transport processes, mediated by membrane carriers, channels or pumps, which were not known at that time, and it ignores inhomogeneities, such as rafts,[3] which may exist in the biological membrane. The rule works fine for all molecules that merely cross the lipid matrix by simple diffusion.

According to this rule, the transmembrane flux density, J, of a membrane-permeating molecule can be predicted if its partition coefficient, K_p, from the aqueous phase into the organic phase, is known. Therefore, Fick's law of diffusion has to be rewritten as Equation (1) (compare also Figure 1):

$$J = -D_M \frac{dc_m}{dx} = -D_M \frac{c_{1m} - c_{2m}}{d}$$
$$J = P_M(c_{2w} - c_{1w}) \quad \text{with } P_M \equiv \frac{K_p D_M}{d} \qquad (1)$$

where D_M, c_{1m}, c_{2m}, c_{1w}, c_{2w}, x, and d are the diffusivity within the organic phase, the concentration of the permeating molecule within the membrane at the first and second interfaces—and their aqueous concentrations at the first and second interfaces—the distance from the first interface, and the membrane thickness, respectively. The term membrane permeability, P_M, is defined based on Equation (1).

Within the last 110 years, thousands of compounds have been tested, and the number of molecules that apparently do not obey Equation (1) is very limited.[4–8] All the exceptions to this rule, which have been reported so far, can be divided into two groups:

i) Substances that may cross the membrane through transient defects. Section 2 is devoted to the most prominent example of substances belonging to this group, namely, the proton.

ii) Substances that do not cross the lipid membrane through transient defects, such as aromatic or simple carboxylic acids, cell-penetrating peptides, and CO_2. Section 3 critically

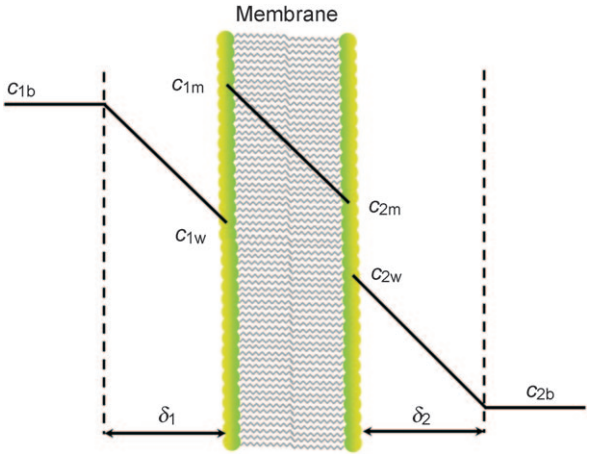

Figure 1. Concentration profile of a lipophilic compound (the partition coefficient $K_p > 1$) within a homogeneous lipid membrane. c_{1b}, c_{2b}, c_{1w}, c_{2w}, c_{1b}, c_{1m}, and c_{2m} denote the solute concentration of the permeable solute in the first (left) bulk solution, in the second (right) bulk solution, in the first aqueous phase adjacent to the bilayer, in the second aqueous phase adjacent to the bilayer, in the lipid phase adjacent to the first compartment, and in the lipid phase adjacent to the second compartment. Unstirred layers, UL, on both sides of the bilayer are denoted as δ. Transport through the bilayer occurs solely by diffusion.

[a] *Dr. A. Missner, Prof. Dr. P. Pohl*
Institut für Biophysik, Johannes Kepler Universität
Altenberger Str. 69, 4040 Linz (Austria)
Fax: (+43) 732-2468-9270
E-mail: peter.pohl@jku.at

re-evaluates these "violations" of the Meyer–Overton rule and shows that Equation (1) may be more robust than has been anticipated.

2. Protons as an Exception to the Meyer–Overton Rule

The main determinant of K_p for ions is their Born energy, that is, the energy that is required to transfer them from the aqueous to the organic phase [Eq. (2)]:

$$\Delta G_{Born} = -\frac{q^2}{8\pi\varepsilon_o r}\left(\frac{1}{\varepsilon_M}-\frac{1}{\varepsilon_W}\right) \quad (2)$$

where the dielectric constants for the lipid phase and water are $\varepsilon_M = 2$ and $\varepsilon_W = 80$, respectively. Considering that the radius r of H_3O^+ is not much different from that of small alkali or halide ions, we would expect that the K_p value of all these ions—and thus their P_M—should be roughly of the same order of magnitude. In contrast, with 10^{-3}–10^{-4} cm s^{-1}, the P_M of protons is about ten orders of magnitude larger.[9–13]

In addition to weak acid/base shuttles (e.g. free fatty acids), transient membrane-spanning water wires have also been suggested to be responsible for the inconsistencies between theoretical and measured data. Facilitated proton translocation by structural diffusion (Grotthuss mechanism) along these water wires implies that proton mass transfer does not occur,[14] since only the isolated protonic charge is moving along the hydrogen-bonded water network (Figure 2). Although no detailed molecular picture is available yet explaining how the excess proton is shared among the water molecules[15,16] or how the required transient membrane defects are formed,[17] the unparalleled speed of Grotthuss diffusion is commonly accepted, as it also underlies lateral migration along membrane surfaces[18] and proton hopping through the membrane channels.[19–21] Since the exceptional rate of structural diffusion is limited to protons, the question arises as to whether other exceptions to the Meyer–Overton rule may exist and if yes, what the underlying mechanism may be.

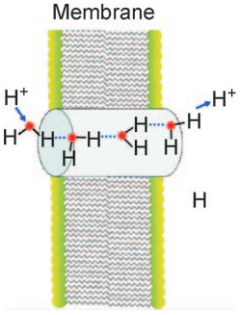

Figure 2. Transient water wires across a lipid bilayer. At one end of a hydrogen-bonded water chain, a proton binds and forms a hydronium (H_3O^+) ion. The "excess" proton charge hops along water molecules, finally being released at the opposite end. This process is thought to be followed by a reorientation of participating water molecules.

3. Exceptions to the Meyer–Overton Rule Unrelated to the Transient Pore Theory

During the last 110 years, a long list of molecules has emerged, all of which were reported to have violated Equation (1). This paragraph focuses on just a few recent examples. These examples do not include molecules crossing the membranes by a flip-flop mechanism, such as long-chain fatty acids or phospholipids. The reason is twofold: i) the flip-flop of charged molecules is known to be facilitated by an increase in mechanical tension accompanied by defect formation in at least one leaflet,[22] and ii) the large K_p value of long-chain fatty acids predicts such a high transport rate[23] that the differences in P_M can hardly be detected with current techniques.[24–26]

3.1. Aromatic Weak Acids

Salicylic acid (SA; p$K_{SA} = 2.75$) is one of the best known agents in the family of aromatic carboxylic acids. The interest in SA has been generated by its activity as an anti-inflammatory agent,[27] its protective role against neurotoxicity,[28] and its potency to reverse obesity- and diet-induced insulin resistance.[29]

Recently, the membrane permeabilities of the SA anion and the protonated SA, $P_{M,SA-}$ and $P_{M,SA}$, were reinvestigated. $P_{M,SA-}$ and $P_{M,SA}$ were found to be equal to 5.4×10^{-9} and 3.5×10^{-7} cm s^{-1}, respectively.[30] This finding violates the Meyer–Overton rule in two respects: i) $P_{M,SA}$ is unreasonably low. From the octanol water partition coefficient $K_p \approx 300$,[31] Equation (1) predicts $P_{M,SA} \approx 1$ cm s^{-1}. ii) The difference between $P_{M,SA-}$ and $P_{M,SA}$ is too small. According to Equation (2), $\Delta G_{Born,A-}$ amounts to about 28 kJ mol^{-1}. Calculating the ratio of the P_M values for the protonated and charged forms of SA, according to Equation (1), reveals [Eq. (3)]:

$$r = \frac{P_{m,AH}}{P_{m,A-}} = \frac{K_{p,AH}}{K_{p,A-}} \approx e^{\Delta G_{Born}/RT} \approx 73000 \quad (3)$$

that is, the difference between $P_{M,SA-}$ and $P_{M,SA}$ should be three orders of magnitude larger than has been reported.[30]

The reason for the discrepancy between theory and experiment becomes evident, if the limitations of the experimental approach are considered. SA uptake into liposomes with a diameter of $d = 200$ nm was monitored by following its complex formation with intravesicular Tb^{3+} (Figure 3). The theoretical $P_{M,SA}$ of 1 cm s^{-1} predicts that the fluorescence of the $SA^- Tb^{3+}$ complex increases exponentially with the time constant τ [Eq. (4)]:

$$\tau = \frac{V}{AP_m} = \frac{\pi d^3}{6\pi d^2 P_m} = \frac{d}{6P_m} \approx 3.4\,\mu s \quad (4)$$

This means that τ is equal to only about 1/100 of the time required for mixing the solutions, even in the best stopped-flow devices currently available on the market. In other words, investigation of SA transport by stopped flow is impossible. Application of the stopped-flow technique is limited to solutes permeating with $P_M < 10^{-2}$ cm s^{-1}. It is noteworthy that Equa-

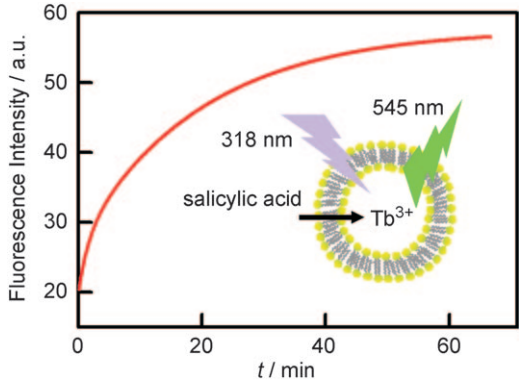

Figure 3. Salicylic acid influx into egg–phosphatidylcholine liposomes was monitored at neutral pH via a luminescence based assay. The Tb^{3+} loaded vesicles were excited at 318 nm and the emission was measured at 545 nm. The reaction was started by adding 9 μM of salicylic acid at time $t = 0$ min. The fluorescence due to complex formation between Tb^{3+} and salicylic acid increased with time (not shown). Shown is a biexponential fit to the data with rate constants of 6 and 0.5 s^{-1}. The data were taken from ref. [30].

tion (4) assumes a constant volume, that is, it does not apply to volume (water) flow.

To prove that SA permeates membranes at the rate predicted by the Meyer–Overton rule, one has to overcome the limited time resolution of kinetic approaches, that is, a steady-state approach would be desirable. It can be realized by planar bilayer experiments as has been shown in the past.[32–34] Since the planar membrane separates two bulky compartments from each other, it would take up to several hours or days until the transmembrane concentration gradient vanishes. In the past, the technique has been criticized for large uncertainties in its quantitative flux estimates arising from near-membrane unstirred layers (ULs). As will be outlined below, exploitation of the scanning electrochemical microscopy solved the problem.

Unstirred layers arise from the nonslip condition near boundaries, that is, even in a vigorously stirred system, stagnant water layers adjacent to the membrane remain. Within this convection-free layers of size δ, transport is solely due to diffusion.[35] The parameter δ is defined in terms of the concentration gradient at the interface [Eq. (5)]:

$$\left.\frac{\partial c}{\partial x}\right|_{x=0} = \frac{c_s - c_b}{\delta} \tag{5}$$

The lack of convection is not to be taken literally. Rather, convection increases gradually, that is, with an increasing distance from the membrane stirring becomes more and more important and after a certain distance, the velocity of convective fluid flow approaches bulk values.[36]

Since unstirred layers act as additional diffusion barriers in series with the membrane, the difference between the bulk concentrations of the permeant ($c_{1b} - c_{2b}$) might remarkably differ from the transmembrane concentration difference ($c_{1w} - c_{2w}$) (compare Figure 1). Denoting the permeabilities of the first and second ULs with $P_{UL,1}$ and $P_{UL,2}$, respectively, the permeability P obtained by flux measurements is equal to [Eq. (6)]:

$$\frac{1}{P} = \frac{1}{P_{UL,1}} + \frac{1}{P_M} + \frac{1}{P_{UL,2}} \tag{6}$$

$P_{UL,1}$ and $P_{UL,2}$ are determined by the UL size δ and the aqueous diffusion coefficient D of the molecules [Eq. (7)]:

$$P_{UL} = \frac{D}{\delta} \tag{7}$$

Visualization of the concentration distribution of the permeating species within the UL by scanning ion-sensitive microelectrodes allows determination of δ, c_{1w}, and c_{2w}. It is, thus, possible to precisely determine both the transmembrane flux and P_M [Eq. (8)]:

$$\begin{aligned} J &= P_{UL,1}(c_{b,1} - c_{w,1}) = P_M(c_{w,1} - c_{w,2}) \\ &= P_{UL,2}(c_{w,2} - c_{b,2}) \end{aligned} \tag{8}$$

without making any additional assumptions about UL effects. Flux measurements are also possible when selective microelectrodes for the permeating species itself are not available. If a fast chemical reaction is initiated, it is sufficient for product concentration to be monitored by electrodes.

SA flux, for example, can be measured since—like any other weak acid or base—it is subject to proton-transfer reactions (Figure 4). Being charged at physiological pH, the vast majority of the SA anions pick up a proton to pass the membrane. This is true both for the "old fashioned" model[32] operating according to the Meyer–Overton rule and for the new stopped-flow-based model according to which the transmembrane diffusion of the deprotonated form was claimed to significantly contrib-

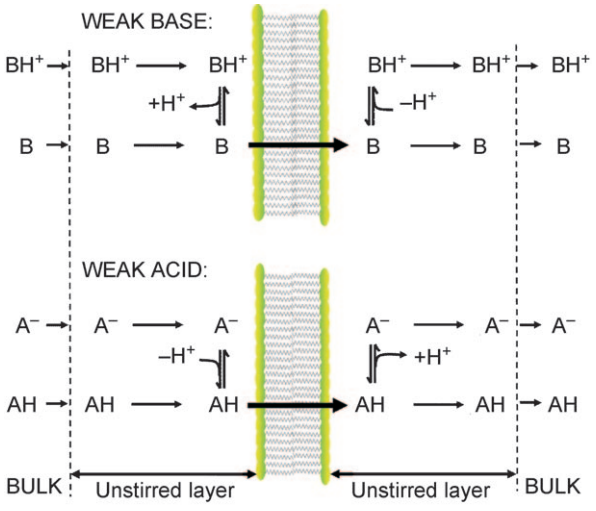

Figure 4. Membrane diffusion of weak acids and bases includes the following steps (from left to right): 1) Diffusion through the left UL; 2) Proton uptake or proton release for weak acids or bases, respectively, at the membrane–water interface to form the neutral form of the weak acid/base; 3) Only the uncharged species passes the lipid bilayer as the charged species is facing the Born energy barrier. 4) Proton uptake or proton release for bases or weak acids, respectively. 5) Finally, all participating molecules pass the right UL by diffusion.

ute to the total SA flux.[30] The proton is released again at the other side of the membrane as the pH value of the solution is several units above the p*K* value of SA. Both the pH increase at the SA donating site of the membrane and the acidification at the receiving site can be measured with pH-sensitive microelectrodes (Figure 5), which scan the UL in the direction perpendicular to the membrane.[6] If almost all permeating molecules are deprotonated in the receiving compartment (pH ≫ pK_{SA}), the transmembrane weak acid flux is directly proportional to the pH gradient at the membrane/water interface [Eq. (9)]:[37]

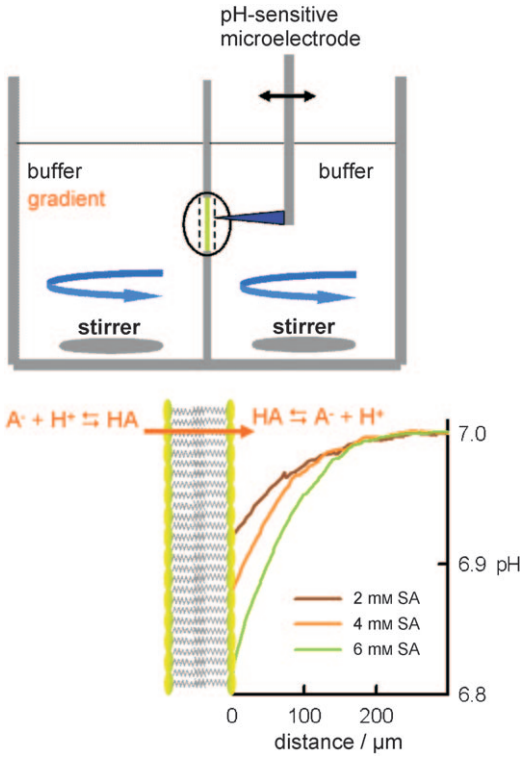

Figure 5. Scanning microelectrode assay for permeability studies. After a stable model membrane has been formed, salicylic acid (SA) is added to one side of the membrane; hereafter referred to as first side. Transmembrane diffusion of SA is followed by proton release in the second compartment because pH > p*K* (compare Figure 4). The resulting tiny pH shift is recorded by moving a microelectrode perpendicular to the membrane. Its magnitude depends both on the distance to the membrane and on concentrations of sodium salicylate (as indicated). Continuous stirring of the buffer solution ensures well-defined ULs on both sides of the membrane. The Figure is modified from ref. [7].

$$j_p = D_{OH}\frac{\Delta[OH^-]}{\delta_{OH}} + D_H\frac{\Delta[H^+]}{\delta_H} + D_B\frac{\beta \times \Delta pH}{\delta_B} \approx D_B\frac{\beta \times \Delta pH}{\delta_B} \quad (9)$$

where D_{OH}, D_H, D_B, and β denote the diffusion coefficients of hydroxyl ions, protons, buffer molecules, and the buffer capacity, respectively. δ_{OH}, δ_H, δ_B indicate the UL thicknesses for hydroxyl ions, protons, and buffer molecules. Please note that all diffusing substances have their own individual δ.[36] At neutral pH, the first two terms of Equation (9) can be neglected. Thus, Equation (9) yields $j_p = 2\times10^{-11}$ mol cm^{-2} s^{-1} for a transmembrane concentration difference of 2 mM salicylate (compare Figure 5). According to Equation (10):

$$P_M = \frac{j_p}{[AH]} \quad (10)$$

where [AH] is the concentration of the protonated SA, we arrive at $P_{M,SA} = 0.2$ cm s^{-1}.[6] This simplified calculation ignores changes in β adjacent to the membrane. A complete mathematical model, which takes into account all the proton-transfer reactions and diffusion processes, indicates that $P_{M,SA} \approx 1.2$ cm s^{-1}.[6] Addition of cholesterol decreases $P_{M,SA}$ to 0.1 cm s^{-1}.[7] With respect to its applicability to solutes with $P_M < 10^{-2}$ cm s^{-1} [compare Eq. (4)], it is not surprising that the stopped-flow approach failed to monitor the well-known effect of cholesterol on D_M [and thus P_M, see Eq. (1)] of small substances.[38]

Planar bilayers also allowed direct determination of $P_{M,SA-}$ with 4×10^{-7} cm s^{-1}[6] from transmembrane current measurements carried out under voltage clamp conditions. That is, if properly measured, both the absolute value of $P_{M,SA}$ and the difference between $P_{M,SA-}$ and $P_{M,SA}$ agree well with what has been predicted by the Meyer–Overton rule.[6,7,32]

3.2. Transport of Short-Chain Carboxylic Acids through Membranes

As the hydrophobicity of carboxylic acids increases with their chain length, acetic acid is, according to the Meyer–Overton rule, expected to diffuse through a lipid bilayer at a lower rate than butanoic or hexanoic acids. Very recently, Grime et al. reported the opposite phenomenon: the most hydrophilic substance exhibited the highest membrane permeability.[39]

In their experiments, the source of the acids was positioned within the UL, 20 µm away from a planar lipid bilayer, and the volume between the place of ejection and the membrane was maintained at a pH below the pK_a of all weak acids (Figure 6). Subsequent to diffusion through the UL and the bilayer, the weak acid released a proton as bulk pH was above pK_a in the receiving compartment. Fluorescence imaging of a water-soluble pH dye revealed that the pH gradient in the second compartment was maximal for the most hydrophilic weak acid, thus suggesting that it encountered the lowest resistance while permeating the membrane.

Since all of the investigated acids had a $K_p \geq 0.49$,[4] the Meyer–Overton rule suggests that they are all fairly membrane-permeable. This also agrees with published data, where P_M ranges from 6.9×10^{-3} to 1.1 cm s^{-1}.[4] Estimates of P_{UL} [Eq. (7)] reveal that $P_M \gg P_{UL}$. The diffusion coefficient of acetic acid, $D = 1.27\times10^{-5}$ cm^2 s^{-1}, and the thickness of the first UL, $\delta_{UL,1} = 20$ µm, result in a permeability of the first UL, $P_{UL,1}$, of 6.35×10^{-3} cm s^{-1}. The second compartment is completely unstirred so that $\delta_{UL,2}$ is equal to the dimensions of that compartment. Taking $\delta_{UL,2} = 2$ mm, we arrive at $P_{UL,2}$ of 6.3×10^{-5} cm s^{-1}.

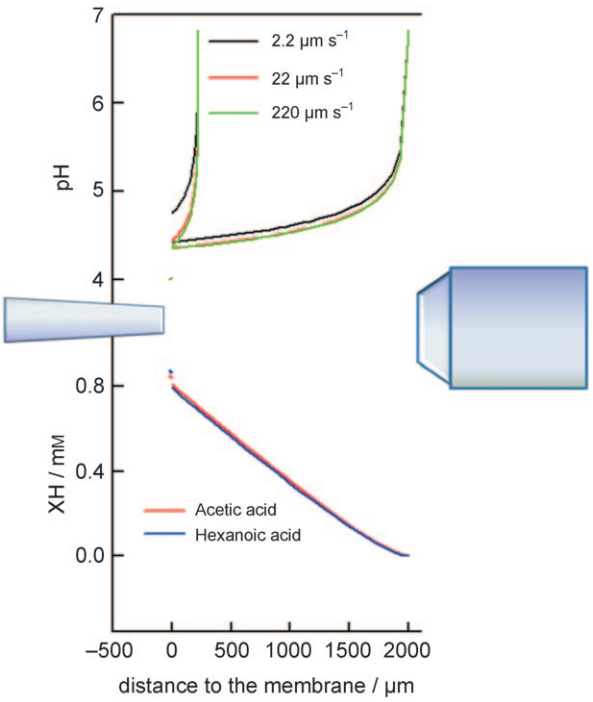

Figure 6. Monitoring membrane diffusion of short-chain carboxylic acids with confocal fluorescence microscopy. The source of the weak acid is shown on the left, the objective of the laser scanning microscope on the right. Instead of presenting the original experimental results, we show theoretical pH (A) and weak acid (B) distributions in the membrane vicinity. The differential equations for the combined processes of diffusion and chemical reaction were solved with respect to the boundary conditions: i) that pH is equal to bulk pH at the edge of the second (right) unstirred layer and equal to 4.0 at the edge of the first (left) unstirred layer, and ii) that total acid concentration (the sum of the anionic and protonated acid concentrations) was equal to 1 mM at the −20 µm boundary and zero at the 220 µm (α) or 2 mm (β) boundary. To show how the profiles change with time, we performed model calculations in which we fixed $\delta_{UL,1}$ to 20 µm and $\delta_{UL,2}$ to 220 (α) or 2000 µm (β). The calculations represent a minor modification of a previously published model.[40] They were carried out analogous to the calculations of bilayer and aquaporin CO_2 permeabilities.[41] A) Varying the permeability coefficient for acetic acid by two orders of magnitude revealed only minor changes in the 2 mm-wide unstirred layer. B) The theoretical concentration distributions of acetic ($P_m = 22\ \mu m\ s^{-1}$) and hexanoic ($P_m = 6.3\ \mu m\ s^{-1}$) acids are very close to each other. In both cases, membrane resistance ($1/P_m$) to acid flux is negligible. The Figure was modified from ref. [8].

Consequently, the overwhelming resistance to acid transport is generated by the UL of the second compartment.[8]

Grime et al. claim that $P_{UL,2} \approx 6.3 \times 10^{-5}\ cm\ s^{-1}$ is not a realistic representation of their experimental situation. They believe that two-dimensional diffusion greatly enhances mass transport in their microelectrochemical system, so that there is no discernible difference in the profiles for 1.5 s and steady state.[42] The argumentation seems to ignore everything that is known about diffusion. The average distance of diffusion after 1.5 s is equal to [Eq. (11)]:

$$\langle x^2 \rangle^{\frac{1}{2}} = \sqrt{2Dt} = \sqrt{2 \cdot 1.27 \cdot 10^{-5}\ cm^2\ s^{-1} \cdot 1.5\ s} = 0.062\ mm \quad (11)$$

Thus, within a 1.5 s time span, an acid molecule crosses the distance between the donating electrode and the membrane, the membrane itself and about 1/20 of the receiving compartment. In case of two or three-dimensional diffusion, the distance travelled normal to the membrane would be even smaller.

Grime et al. claim that at $t = 1.5$ s a stationary concentration distribution is reached. But what would prevent the vast majority of the molecules from diffusing beyond this imaginary boundary reached at 1.5 s? A fundamental law of thermodynamics requires that entropy is maximized. Consequently, diffusion has to continue. Continuous diffusion continuously changes the concentration gradient at the membrane water interface [compare Eq. (5)] in the receiving compartment. This is true even if we assume that i) changes of c_w are so small that they can be ignored (because both pH and the acid concentration in the donating compartment are kept constant) and that ii) c_b is zero for the first minutes of the experiment. However, due to continuous diffusion, the distance from the membrane where c_b = zero increases continuously. If so, the flux through the UL layer will change with time, as does the flux through the membrane, since both have to be equal to each other [Eq. (12)]:

$$J_M = J_{UL,2} = D\frac{c_s - c_b}{\delta} \quad (12)$$

The fact that δ grows with time in the absence of stirring was illustrated over 30 years ago by a laser interferometrical study.[43] The half time $t_{1/2}$ required to reach the steady state can be used to estimate δ [Eq. (13)]:[35]

$$t_{1/2} = 0.38\ \frac{\delta_{UL,2}^2}{D} \quad (13)$$

For $\delta = 2$ mm, $t_{1/2}$ is equal to 1200 s. Since c_b was not fixed in the experiments of Grime et al., diffusion of the molecules to the edge of the UL would continue long after 2400 s have passed. It acts to augment c_b so that there are no stationary concentration profiles until equilibrium is reached.

To show the effect of the UL size, we performed model calculations in which we fixed $\delta_{UL,1}$ to 20 µm and $\delta_{UL,2}$ to 220 or 2000 µm. These profiles should have evolved, one subsequent to the other, in the system of Grime et al. due to the absence of convection. For the larger $\delta_{UL,2}$, the pH distributions for acids with P_M of 22 and 220 $\mu m\ s^{-1}$ are indistinguishable. This result confirms the prediction that $P_M \gg P_{UL}$.

Grime et al. also performed model calculations to support their theory.[39,42] However, they did not offer an explanation as to why the molecules did not diffuse beyond an imaginary boundary set to 220 µm in their calculations. They also failed to explain, why the model calculations where restricted to a box size < 700 µm, although its real size was 2000 µm in the x direction.

We monitored pH profiles generated in the ULs by acetic acid diffusion 15 years ago. In contrast to Grime et al., our bulk solutions were stirred, buffer molecules were present and ac-

counted for by the analytical model, and, most importantly, bulk pH was basic to establish a situation where membrane diffusion is rate limiting.[40] Membrane transport becomes rate-limiting at pH 8, because the concentration of the membrane-impermeable anion exceeds the one of the protonated species thousand-fold, and because the anion contributes to the membrane flux of the protonated species by picking up a proton at the interface. P_M determination unbiased by UL effects revealed 6.9×10^{-3} cm s^{-1},[40] that is, a value that exceeds that determined by Grime et al. threefold. The P_M value agreed very well with results from tracer experiments of Walter and Gutknecht. In perfect agreement with the Meyer–Overton rule, the same authors found 1.1 cm s^{-1} for hexanoic acid.[31] It is thus safe to conclude that the study by Grime et al.[39,42] was hampered by UL effects. UL limitations led to severe underestimations of P_M for all carboxylic acids in their system.

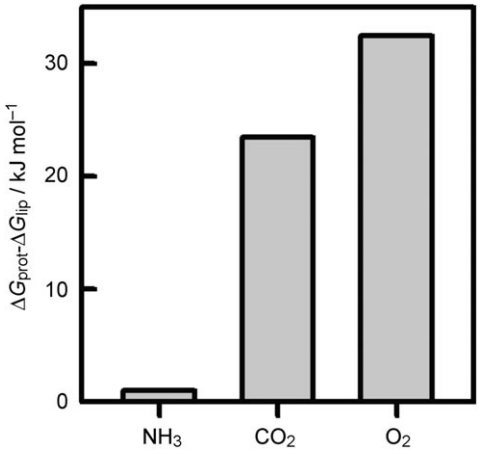

Figure 7. Difference in the free-energy barriers of the aquaporin channel and lipid pathways $\Delta G_{prot}-\Delta G_{lip}$. For all the gases, diffusion through a pure dipalmitoyl phosphatidylcholine membrane is energetically favourable. Data are taken from a molecular dynamics simulation.[51]

3.3. Gas Transport through Membranes and Membrane Channels

The interest in channels that may facilitate gas transport has dramatically increased in recent years: The structure of a putative ammonia channel has been determined,[44] aquaporins were found to conduct ammonia[45] and reported to provide a CO_2 pathway.[46,47] Messengers, such as H_2S[48] and NO, are also thought to be channelled by membrane proteins.[49,50]

It is important to note that membrane channels facilitate transport by decreasing the otherwise large energy barrier for solute movement through the hydrophobic membrane interior. Ion channels, for example, decrease ΔG_{Born} by providing an environment with an increased ε. Gas channels must also act to increase the partitioning of volatile molecules into the membrane. It is hard to imagine how this general rule works in the case of a molecule such as CO_2 with $K_p \geq 1$. The Meyer–Overton rule would predict that these molecules permeate the membrane nearly as fast as they would permeate a water layer of the same thickness of 5 nm. In this case, the membrane cannot act as barrier to CO_2. Passing a CO_2-selective channel would require interactions of the volatile solute with the channel wall, which would merely tend to increase the transport barrier. These theoretical considerations are reflected by molecular dynamics simulations predicting that the passage through a phosphatidyl choline bilayer is less costly than the passage through aquaporins for CO_2 and O_2.[51] Due to its $K_p \ll 1$, the energetic expenses for NH_3 diffusion through the bilayer and the proteinacous pore were roughly equal to each other (Figure 7).

In contrast to the predictions of the Meyer–Overton rule, evidence in favour of facilitated gas transport has been reported for over three decades.[52] Because of its high abundance in gas-exchanging tissues,[53] a physiological role of the water channel protein (aquaporin-1) in CO_2 or O_2 transport was suggested.[54] Evidence was provided by experiments on aquaporin-1 or NtAQP1 (tobacco aquaporin) over-expressing *Xenopus* oocytes which showed faster intracellular acidification (pH_i) rates compared to wild-type oocytes when exposed to an elevated external CO_2 concentration.[46,55] These experiments are not convincing, because the existence of both extracellular and intracellular ULs has been ignored. These ULs are likely to extend over at least 100 μm on each side of the membrane. According to Equation (6), this results in a $P_{UL,1}$ of 2×10^{-3} cm s^{-1} for the external UL and a $P_{UL,2}$ of $\approx10^{-4}$ cm s^{-1} for the internal UL. The difference between $P_{UL,1}$ and $P_{UL,2}$ results from a fourfold reduction of the solute diffusion coefficient in cytoplasm versus saline.[56,57] Detection of an aquaporin-mediated increase in P_M would require that P_M of the lipid matrix is $\leq10^{-4}$ cm s^{-1}, that is, several orders of magnitude below the value measured with a tracer technique for planar lipid membranes.[58] In the absence of any experimental proof for this very unlikely anticipation, *Xenopus* oocytes may not be used for P_M measurements of CO_2.

Recent time-lapse experiments with pH microelectrodes placed within the external UL, at a distance of 40 μm to the *Xenopus* oocyte surface, revealed that some aquaporin channels specifically transport CO_2 and some are selective to either NH_3 or NH_4^+.[59] As a criterion, the extreme excursions of pH caused by CO_2 influx were taken at the microelectrode position. It is not clear, how these excursions are related to P_M or the CO_2 flux. Since the method does not allow estimation of the interfacial CO_2 concentrations c_{1w} and c_{2w}, its accuracy is also hampered by UL effects. That is, detection of the aquaporin-mediated increase in P_M would require that P_M of the oocyte membrane should be around 10^{-4} cm s.$^{-1}$ Since proof for this unlikely hypothesis is missing, the interpretation of the differences observed for specific aquaporins in the extreme pH excursions is not clear. One possibility is that ion channels endogenous to *Xenopus* oocytes are drastically altered due to the expression of channel proteins, as has been previously reported.[60]

Evidence of aquaporin-mediated CO_2 transport has also been obtained with stopped-flow experiments on proteoliposomes. Reconstitution of purified human aquaporin-1 (hAQP1) caused a fourfold increase in the rate of intravesicular acidification (Figure 8) observed in the presence of an increased external CO_2 concentration.[47] A subsequent study confirmed this

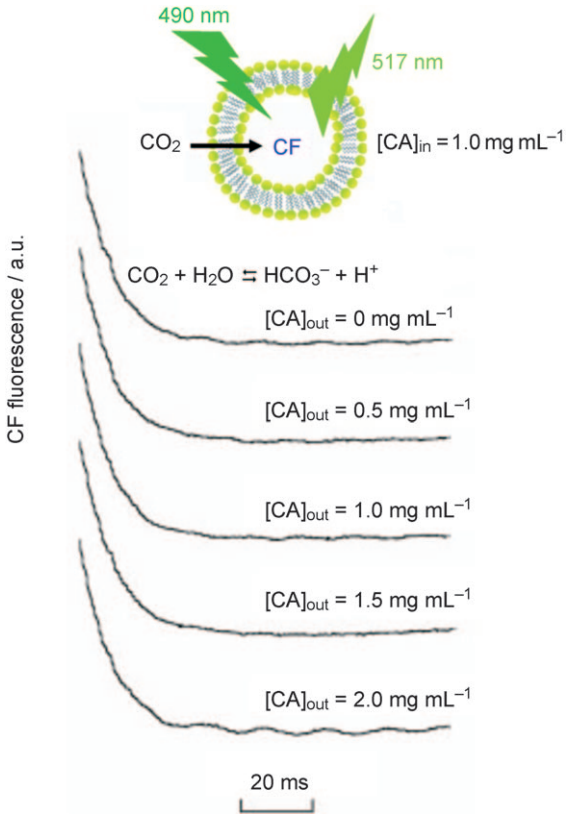

Figure 8. CO_2 diffusion into lipid vesicles reconstituted with aquaporin-1. CO_2 uptake into the vesicles is followed by CO_2 hydration (catalyzed by carbonic anhydrase, CA) and proton release. The resulting intravesicular acidification is monitored via the pH-sensitive dye carboxyfluorescein (CF). CA catalyzes also the dehydration of $H_2CO_3/HCO_3^-/CO_3^{2-}$ which otherwise would be very slow. The lack of effect of CA addition to the external solution (taken from ref. [61]) indicates that the kinetics of the fluorescence signal does not mirror neither the kinetics of the dehydration nor the kinetics of the much faster CO_2 transport. Rather, it reflects the kinetics of a much slower process: the kinetics of mixing proteoliposome- and CO_2-containing solutions.

observation. However, CO_2 flux through aquaporin-containing vesicles was independent on the concentration of external carbonic anhydrase.[61] In the absence of carbonic anhydrase, the reactions [Eqs. (14)]:

$$CO_2 + H_2O \underset{k_1}{\overset{k_{-1}}{\rightleftharpoons}} H_2CO_3 \;;\; CO_2 + OH^- \underset{k_2}{\overset{k_{-2}}{\rightleftharpoons}} H_2CO_3^- \qquad (14)$$

would proceed with $k_1 \approx 3.7\times10^{-2}\ s^{-1}$ and $k_2 \approx 2\times10^{-4}\ s^{-1}$, that is, CO_2 would form much slower than it is transported through the membrane.[58] Consequently, the change in the intravesicular acidification rate observed upon aquaporin reconstitution[47] cannot be interpreted in terms of a facilitated CO_2 transport by these channels.[61] The lack of an effect of carbonic anhydrase may indicate that CO_2 transport into vesicles is generally limited by CO_2 diffusion towards the vesicles through near-membrane ULs.[61] However, a realistic estimation of the UL effects reveals that the combined permeabilities of the external and internal ULs, δ_{out} and δ_{in} in size, is equal to [Eq. (15)]:

$$P_{UL} = \frac{D_{CO_2}}{\delta_{in} + \delta_{out}} = \frac{2.9\cdot10^{-9}\ m^2\ s^{-1}}{(120+60)\ nm} = 1.6\ cm\ s^{-1} \qquad (15)$$

P_{UL} is, thus, much larger than the estimates given for $P_{M,CO2} \approx 1.2\times10^{-3}\ cm\,s^{-1}$ in ref. [61] and $\approx 1.9\times10^{-3}\ cm\,s^{-1}$ in ref. [47]. Consequently, limitations by the ULs were not responsible for the vast underestimation of $P_{M,CO2}$. Rather, it is the dead time of the stopped-flow apparatus which limits the observable transport rate [compare Eq. (4)]. If we assume that the whole process of pumping and mixing of the vesicle-containing and the CO_2-donating solutions takes about 1 ms, and that the proteoliposomes have a diameter of about 120 nm, calculation according to Equation (4) exactly predicts the reported $P_{M,CO2}$ value. Larger $P_{M,CO2}$ values cannot be measured since the time resolution of the stopped-flow approach is insufficient. Thus, it cannot be used to show that the lipid membrane is a barrier to CO_2 transport, that is, to disprove the Meyer–Overtone rule. Similarly, stopped-flow experiments cannot be used to demonstrate that aquaporins increase the CO_2-transport rate.

A third line of evidence in favour of aquaporin-mediated CO_2 transport has been obtained by a mass spectrometric technique.[62,63] Red blood cells were introduced into a solution of ^{18}O-labeled HCO_3^-. Cellular uptake of $C^{18}O^{16}O$ was continuously monitored by mass spectrometric measurements of the extracellular concentration of $C^{18}O^{16}O$. Its rate decreased three- to fourfold when both the Rh protein complex and aquaporin-1 were neither expressed nor in a functionally active state. The authors proved that the intraerythrocytic carbonic anhydrase activity was high. Unfortunately, they neither checked for carbonic anhydrase IV activity localized on the exterior surface of human erythrocytes[64] nor did they add carbonic anhydrase into the external solution. Thus, it is not clear whether the process according to Equation (14) was rate-limiting. But even if we assume that CO_2 formation was not the limiting transport process, diffusion through the extracellular and intracellular ULs surely was. Ammonia permeability studies of erythrocyte membrane by ^{14}N and ^{15}N saturation transfer NMR spectroscopy revealed a P_{UL} of the red blood cells of about $10^{-3}\ cm\,s^{-1}$.[65] Since the diffusion coefficients of ammonia and CO_2 are similar, the P_{UL} values for ammonia and CO_2 should also be similar. It may be possible to achieve an up to tenfold increase in P_{UL} by vigorous stirring. This limit cannot be further extended if it is considered that the internal UL has a size of $\delta_{in} \geq 2\ \mu m$, which alone contributes a $P_{UL,2}$ of $\approx D_{CO2,cytoplasm}/\delta_{in} \approx D_{CO2,saline}/4\,\delta_{in} \approx 3\times10^{-2}\ cm\,s^{-1}$ due to the lack of intracellular convection. That is, $P_{UL,2}$ is about two orders of magnitude smaller then the P_M of $3\ cm\,s^{-1}$,[41] that is, ULs are clearly rate-limiting for CO_2 transport.

Endeward and Gros arrived at a seemingly much larger P_{UL} when analysing the effect of increased kinematic viscosity ν of the suspension on the $C^{18}O^{16}O$ uptake by red blood cells.[66] Their key finding was a linear dependence of $1/P$ on ν. This was anticipated, since [Eq. (16)]:

$$\frac{1}{P_{UL,1}} = \frac{\delta_{out}}{D_{CO_2}} = \delta_{out}\frac{6\pi\rho\nu r_{CO2}}{kT} \qquad (16)$$

where r_{CO2}, ρ, k, and T are the radius of the CO_2 molecule, the density, the Boltzmann constant, and the absolute temperature, respectively. Equation (16) states that $1/P_{UL} \sim \nu$ for constant δ_{out}. In contrast, the authors attributed the linear rise in $1/P_{UL}$ exclusively to a linear increase in δ_{out}. The following step in the erroneous line of interpretations was that δ_{out} is a linear function of ν.[66] It contrasts with commonly accepted results from a mathematical analysis of the problem derived for special geometries, which led to [Eq. (17)]:[67,68]

$$\delta_{out} \sim \left(\frac{D}{v}\right)^{1/3} \left(\frac{v}{\alpha}\right)^{1/2} \quad (17)$$

where α is a stirring parameter. The validity of Equation (17) for arbitrary geometries has been demonstrated experimentally by showing that the UL thicknesses of two substances A and B are related to their diffusion coefficients, as shown in Equation (18):[36]

$$\frac{\delta_A}{\delta_B} = \sqrt[3]{\frac{D_A}{D_B}} \quad (18)$$

Consequently, it is safe to conclude that the approach by Endeward and Gros[66] is not suitable for the determination of δ_{out}. The inverse proportionality $1/P_{UL} \sim \nu$ indicates that either intracellular or extracellular ULs limit CO_2 uptake into red blood cells. Thus, any contribution membrane channels may make under these conditions is physiologically irrelevant (and immeasurable).

Reliable measurements of $P_{M,CO2}$ can be made in the steady state using planar lipid bilayers. Gutknecht et al. measured the diffusion of ^{14}C-labeled CO_2 from a donating compartment through the planar bilayer into the receiving compartment.[58] They tried to get rid of the UL limitations by increasing pH to 9–10 and by increasing the buffer capacity. Although, the ratio $[HCO_3^- + CO_3^{2-}]:[CO_2]$ is larger than 1000 under these conditions, transport through the membrane is still not rate-limiting,[41] so that their permeability estimate of 0.35 cm s^{-1} was biased by UL effects.

Instead of minimizing UL effects or correcting for them, they may actually be utilized to measure transport.[40,69] Proton uptake or release, which accompanies CO_2 transport, can be monitored using scanning microelectrodes.[41] Figure 9 shows spatially resolved pH shifts adjacent to planar membranes obtained for three different transmembrane CO_2 gradients. These profiles allow calculation of $P_{M,CO2}$, since all relevant chemical reactions and diffusion processes can easily be taken into account [Eqs. (19) and (20)]:

$$J_i^{cis}(x) = -D_i \frac{dc_i^{cis}(x)}{dx} \; R_i(c^{cis}(x)) = \frac{dJ_i^{cis}(x)}{dx} \quad (19)$$

$$J_i^{trans}(x) = -D_i \frac{dc_i^{trans}(x)}{dx} \; R_i(c^{trans}(x)) = \frac{dJ_i^{trans}(x)}{dx} \quad (20)$$

where i denotes the participating species: 1 = H^+, 2 = OH^-, 3 = A^-, 4 = AH, 5 = CO_2, 6 = HCO_3^-, 7 = CO_3^{2-}, 8 = H_2O (A^- and AH are buffering molecules). R_i is the specific local rate of expenditure. At the membrane–water boundary, all fluxes (except for J_5) are set to zero [Eq. (10)]:

$$J_1 = J_2 = J_3 = J_4 = J_6 = J_7 = J_8 = 0; \quad J_5 = J \quad (21)$$

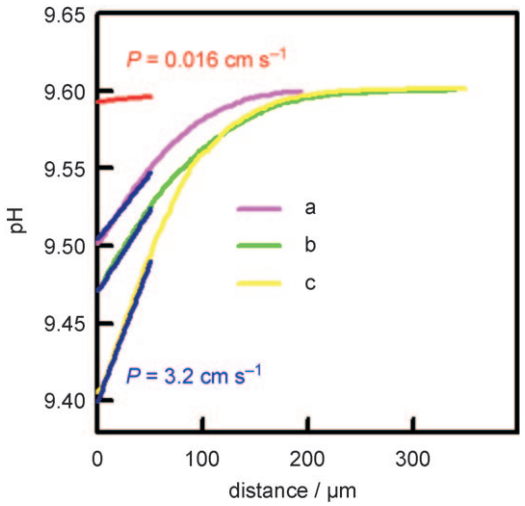

Figure 9. CO_2 diffusion through planar lipid bilayers. Acidification of the receiving compartment is monitored by scanning pH microelectrodes. Experimentally obtained pH profiles for three different gradients are shown: a) 8 mM HCO_3^- plus 3.2 mM CO_3^{2-}; b) 11 mM HCO_3^- plus 4.4 mM CO_3^{2-}; c) 24 mM HCO_3^- plus 9.6 mM CO_3^{2-} (at pH 9.6). The theoretical curves (dark blue) were fitted to the measured profiles, thus leading to a CO_2 membrane permeability of $P_M = 3.2$ cm s.$^{-1}$ In contrast, the red curve shows a "misfit" for $P_M = 0.016$ cm s.$^{-1}$ The Figure was taken from ref. [41].

The model was used to fit the first 50 µm of the experimental pH profiles (Figure 9), thereby yielding a lower limit for the CO_2 membrane permeability of $P_{M,CO2} = 3.2$ cm s^{-1}.[41] Thus, CO_2 transport is so fast that a physiological and significant contribution of membrane-embedded CO_2 channels is elusive.

This result agrees nicely with qualitative predictions by the Meyer–Overton rule and with conclusions from MD simulations, whereby the energy barrier for CO_2 permeation through the lipid bilayer is much smaller than the energy barrier for diffusion through aquaporins.[51] The same MD calculations also found that the energy barriers for NH_3 diffusion through the proteinaceous and lipidic pathways were similar. In agreement with this theoretical analysis, our scanning microelectrode approach revealed that aquaporin-8 is incapable of facilitating NH_3 transport if the channel is reconstituted into pure phosphatidylcholine bilayers.[45]

In contrast, aquaporin-8 provides a physiologically important NH_3 pathway if embedded into a sphingomyelin/cholesterol containing membrane.[45] This finding is easy to understand if we assume that the energy barrier offered by these membranes is about 20 kJ mol^{-1} larger for small molecules (as an upper limit) than of pure phosphatidyl choline membranes.[70] In this case, the aquaporin provides an energetically favourable pathway (Figure 7). However, for CO_2 transport, the situation does not change. According to molecular dynamics simula-

tions, passing the channel still requires more energy than passing the membrane (Figure 7).

Investigations of gas transport through planar bilayers by scanning microelectrodes can be combined with electrophysiological techniques. This has the advantage that the molecular species which actually passes the channel can be identified. For example, evidence for both NH_3 and NH_4^+ transport by aquaporin-8 was reported.[71] However, neither the underlying oocyte experiments nor reconstitution of the channel into vesicles[72] allowed resolving whether NH_4^+ transport occurred through the aquaporin itself or due secondary effects related to rapid NH_3 transport. Simultaneous ion and ammonia flux measurements through planar bilayers revealed perfect NH_3 selectivity, that is, ammonia transport by reconstituted aquaporin-8 is electrically silent.[45]

The high aquaporin abundance in virtually every tissue that transports O_2 and CO_2 at high levels, suggests that these channels may play a physiologically significant role—if not as a CO_2 pathway, at least as an O_2 channel. In contrast, if we assume that i) O_2, NH_3, and CO_2 have comparable membrane diffusivities, and that ii) the Meyer–Overton rule applies, we arrive at the prediction that [Eq. (22)]:

$$P_O \approx P_{NH3} K_{p,O}/K_{p,NH3} \approx P_{CO2} K_{p,O}/K_{p,CO2} \approx 10\ cm\,s^{-1} \quad (22)$$

where $K_{p,O} \approx 2$,[73,74] $K_{p,CO2} \approx 1.5$,[75] $K_{p,NH3} \approx 0.002$,[4] $P_{NH3} = 0.016\ cm\,s^{-1}$,[76] and $P_{CO2} = 3.2\ cm\,s^{-1}$;[41] that is, the large background permeability of the lipid bilayer would render transport facilitation by membrane channels impossible. In line with these considerations, P_O for model membranes has been estimated by ESR based O_2 membrane concentration and mobility measurements to be equal to 210–230 $cm\,s^{-1}$ (at 37–45 °C) in the absence of cholesterol.[73,74] Even if we assume that this value drops to 190 $cm\,s^{-1}$ at room temperature for a fluid membrane, it is still not compatible with the view that the bilayer limits O_2 transport.

Direct P_O permeability measurements have been carried out on planar bilayers. Therefore, singlet oxygen, $^1O_2$, was released from a photosensitizer adsorbed to the second leaflet and the damage of target molecules bound either to the second or the first leaflets was observed.[77] The dependence of the reaction rate on the sidedness of the target indicated that the $^1O_2$ concentrations ($[^1O_2]$) on the first and second membrane interfaces were different. Calculation of the individual reaction rates allowed calculation of the transmembrane $^1O_2$ concentration difference. Since this approach ensures immediate access to the interfacial concentrations c_{1w} and c_{2w}, subsequent calculation the bilayer permeability to $^1O_2$ is not biased by UL effects. Although the resulting value of $\geq 2\ cm\,s^{-1}$ is much smaller than the ESR-based estimate, it rules out the possibility that the membrane acts as a barrier to $^1O_2$ diffusion. Consequently, facilitation of $^1O_2$ or O_2 transport by aquaporins is impossible (compare also Figure 7).

4. Conclusions

All of the reported violations of the Meyer–Overton rule for carboxylic acid and gas transport did not withstand critical evaluation. The 110-year-old rule survived the test of time. We are convinced that this conclusion thus holds true for most of the remaining cases which were not discussed here. For example, simple membrane diffusion of cell-penetrating peptides[78] can be ruled out for energetic reasons: how would a molecule that bears more than five positive net charges overcome the Born energy barrier [Eq. (2)]? In light of this, recent reports excluding endocytosis as an uptake mechanism do not appear convincing.[79] Since passive membrane diffusion of peptides has long been known as impossible,[80,81] what else can possibly be offered as a transport mechanism?

Acknowledgements

We thank Quentina Beatty for proofreading the manuscript. The project was supported by the Austrian Science Fonds (FWF W1201-N13).

Keywords: electrochemical microscopy · gas transport · membranes · Meyer–Overtone rule · unstirred layers

[1] H. Meyer, *Arch. Exp. Pathol. Pharmakol.* **1899**, *42*, 109–118.
[2] E. Overton, *Studien über die Narkose*, Fischer, Jena, **1901**.
[3] L. J. Pike, *J. Lipid Res.* **2006**, *47*, 1597–1598.
[4] A. Walter, J. Gutknecht, *J. Membr. Biol.* **1986**, *90*, 207–217.
[5] Q. Al-Awqati, *Nat. Cell Biol.* **1999**, *1*, E201–E202.
[6] S. M. Saparov, Y. N. Antonenko, P. Pohl, *Biophys. J.* **2006**, *90*, L86–L88.
[7] A. Missner, A. Horner, P. Pohl, *Biochim. Biophys. Acta* **2008**, *1778*, 2154–2156.
[8] A. Missner, P. Kugler, Y. N. Antonenko, P. Pohl, *Proc. Natl. Acad. Sci. USA* **2008**, *105*, E123.
[9] J. W. Nichols, D. W. Deamer, *Proc. Natl. Acad. Sci. USA* **1980**, *77*, 2038–2042.
[10] D. W. Deamer, J. W. Nichols, *Proc. Natl. Acad. Sci. USA* **1983**, *80*, 165–168.
[11] D. W. Deamer, J. Bramhall, *Chem. Phys. Lipids* **1986**, *40*, 167–188.
[12] J. Gutknecht, *Proc. Natl. Acad. Sci. USA* **1987**, *84*, 6443–6446.
[13] S. Paula, A. G. Volkov, A. N. Vanhoek, T. H. Haines, D. W. Deamer, *Biophys. J.* **1996**, *70*, 339–348.
[14] N. Agmon, *Chem. Phys. Lett.* **1995**, *244*, 456–462.
[15] D. Marx, M. E. Tuckerman, J. Hutter, M. Parrinello, *Nature* **1999**, *397*, 601–604.
[16] M. E. Tuckerman, D. Marx, M. Parrinello, *Nature* **2002**, *417*, 925–929.
[17] S. J. Marrink, F. Jahnig, H. J. Berendsen, *Biophys. J.* **1996**, *71*, 632–647.
[18] S. Serowy, S. M. Saparov, Y. N. Antonenko, W. Kozlovsky, V. Hagen, P. Pohl, *Biophys. J.* **2003**, *84*, 1031–1037.
[19] D. G. Levitt, S. R. Elias, J. M. Hautman, *Biochim. Biophys. Acta* **1978**, *512*, 436–451.
[20] F. Mark, R. Pomes, B. Roux, *Biophys. J.* **2000**, *79*, 2840–2857.
[21] S. Cukierman, *Front. Biosci.* **2003**, *8*, S1118–S1139.
[22] R. M. Raphael, R. E. Waugh, *Biophys. J.* **1996**, *71*, 1374–1388.
[23] E. E. Pohl, A. M. Voltchenko, A. Rupprecht, *Biochim. Biophys. Acta Biomembr.* **2008**, *1778*, 1292–1297.
[24] F. Kamp, J. A. Hamilton, *Proc. Natl. Acad. Sci. USA* **1992**, *89*, 11367–11370.
[25] E. E. Pohl, U. Peterson, J. Sun, P. Pohl, *Biochemistry* **2000**, *39*, 1834–1839.
[26] J. P. Kampf, D. Cupp, A. M. Kleinfeld, *J. Biol. Chem.* **2006**, *281*, 21566–21574.
[27] R. B. Gaynor, M. J. Yin, Y. Yamamoto, *Nature* **1998**, *396*, 77–80.
[28] M. Grilli, M. Pizzi, M. Memo, P. Spano, *Science* **1996**, *274*, 1383–1385.

[29] M. Yuan, N. Konstantopoulos, J. Lee, L. Hansen, Z. W. Li, M. Karin, S. E. Shoelson, *Science* **2001**, *293*, 1673–1677.
[30] A. V. Thomae, H. Wunderli-Allenspach, S. D. Kramer, *Biophys. J.* **2005**, *89*, 1802–1811.
[31] A. Walter, J. Gutknecht, *J. Membr. Biol.* **1984**, *77*, 255–264.
[32] J. Gutknecht, D. C. Tosteson, *Science* **1973**, *182*, 1258–1261.
[33] A. Walter, D. Hastings, J. Gutknecht, *J. Gen. Physiol.* **1982**, *79*, 917–933.
[34] P. Pohl, E. H. Rosenfeld, R. Millner, *Biochim. Biophys. Acta* **1993**, *1145*, 279–283.
[35] P. H. Barry, J. M. Diamond, *Physiol. Rev.* **1984**, *64*, 763–872.
[36] P. Pohl, S. M. Saparov, Y. N. Antonenko, *Biophys. J.* **1998**, *75*, 1403–1409.
[37] M. P. Borisova, L. N. Ermishkin, E. A. Liberman, A. Y. Silberstein, E. M. Trofimov, *J. Membr. Biol.* **1974**, *18*, 243–261.
[38] A. V. Thomae, T. Koch, C. Panse, H. Wunderli-Allenspach, S. D. Kramer, *Pharm. Res.* **2007**, *24*, 1457–1472.
[39] J. M. Grime, M. A. Edwards, N. C. Rudd, P. R. Unwin, *Proc. Natl. Acad. Sci. USA* **2008**, *105*, 14277–14282.
[40] Y. N. Antonenko, G. A. Denisov, P. Pohl, *Biophys. J.* **1993**, *64*, 1701–1710.
[41] A. Missner, P. Kugler, S. M. Saparov, K. Sommer, J. C. Matthai, M. L. Zeidel, P. Pohl, *J. Biol. Chem.* **2008**, *283*, 25340–25347.
[42] J. M. A. Grime, M. A. Edwards, P. R. Unwin, *Proc. Natl. Acad. Sci. USA* **2008**, *105*, E124.
[43] D. Lerche, *J. Membr. Biol.* **1976**, *27*, 193–205.
[44] S. Khademi, J. O'Connell III, J. Remis, Y. Robles-Colmenares, L. J. Miercke, R. M. Stroud, *Science* **2004**, *305*, 1587–1594.
[45] S. M. Saparov, K. Liu, P. Agre, P. Pohl, *J. Biol. Chem.* **2007**, *282*, 5296–5301.
[46] N. L. Nakhoul, B. A. Davis, M. F. Romero, W. F. Boron, *Am. J. Physiol.* **1998**, *274*, C543–C548.
[47] G. V. Prasad, L. A. Coury, F. Finn, M. L. Zeidel, *J. Biol. Chem.* **1998**, *273*, 33123–33126.
[48] J. K. Lee, D. Kozono, J. Remis, Y. Kitagawa, P. Agre, R. M. Stroud, *Proc. Natl. Acad. Sci. USA* **2005**, *102*, 18932–18937.
[49] M. Herrera, N. J. Hong, J. L. Garvin, *Hypertension* **2006**, *48*, 157–164.
[50] M. Herrera, J. L. Garvin, *Am. J. Physiol. Am. J. Physiol. Renal Physiol.* **2007**, *292*, F1443–F1451.
[51] J. S. Hub, B. L. de Groot, *Proc. Natl. Acad. Sci. USA* **2008**, *105*, 1198–1203.
[52] D. N. Silverman, C. Tu, G. C. Wynns, *J. Biol. Chem.* **1976**, *251*, 4428–4435.
[53] L. S. King, D. Kozono, P. Agre, *Nat. Rev. Mol. Cell Biol.* **2004**, *5*, 687–698.
[54] W. F. Boron, *J. Am. Soc. Nephrol.* **2006**, *17*, 2368–2382.
[55] N. Uehlein, C. Lovisolo, F. Siefritz, R. Kaldenhoff, *Nature* **2003**, *425*, 734–737.
[56] K. Luby-Phelps, *Int. Rev. Cytol.* **1999**, *192*, 189–221.
[57] E. Dauty, A. S. Verkman, *J. Biol. Chem.* **2005**, *280*, 7823–7828.
[58] J. Gutknecht, M. A. Bisson, D. C. Tosteson, *J. Gen. Physiol.* **1988**, *69*, 779–794.
[59] R. Musa-Aziz, L. M. Chen, M. F. Pelletier, W. F. Boron, *Proc. Natl. Acad. Sci. USA* **2009**, *106*, 5406-5411.
[60] K. Shimbo, D. L. Brassard, R. A. Lamb, L. H. Pinto, *Biophys. J.* **1995**, *69*, 1819–1829.
[61] B. X. Yang, N. Fukuda, A. van Hoek, M. A. Matthay, T. H. Ma, A. S. Verkman, *J. Biol. Chem.* **2000**, *275*, 2686–2692.
[62] V. Endeward, R. Musa-Aziz, G. J. Cooper, L. M. Chen, M. F. Pelletier, L. V. Virkki, C. T. Supuran, L. S. King, W. F. Boron, G. Gros, *FASEB J.* **2006**, *20*, 1974–1981.
[63] V. Endeward, J. P. Cartron, P. Ripoche, G. Gros, *FASEB J.* **2007**, *22*, 1–11.
[64] P. J. Wistrand, N. D. Carter, C. W. Conroy, I. Mahieu, *Acta Physiol. Scand.* **1999**, *165*, 211–218.
[65] R. J. Labotka, P. Lundberg, P. W. Kuchel, *Am. J. Physiol.* **1995**, *268*, C686–C699.
[66] V. Endeward, G. Gros, *J. Physiol.* **2009**, *587*, 1153–1167.
[67] T. J. Pedley, *J. Fluid Mech.* **1980**, *101*, 843–861.
[68] V. G. Levich, *Physicochemical hydrodynamics*, Prentice-Hall, Englewood Cliffs, **1962**.
[69] P. Pohl, Y. N. Antonenko, E. H. Rosenfeld, *Biochim. Biophys. Acta Biomembr.* **1993**, *1152*, 155–160.
[70] A. V. Krylov, P. Pohl, M. L. Zeidel, W. G. Hill, *J. Gen. Physiol.* **2001**, *118*, 333–340.
[71] L. M. Holm, T. P. Jahn, A. L. Moller, J. K. Schjoerring, D. Ferri, D. A. Klaerke, T. Zeuthen, *Pfluegers Arch.* **2005**, *450*, 415–428.
[72] K. Liu, H. Nagase, C. G. Huang, G. Calamita, P. Agre, *Biol. Cell* **2006**, *98*, 153–161.
[73] W. K. Subczynski, J. S. Hyde, A. Kusumi, *Proc. Natl. Acad. Sci. USA* **1989**, *86*, 4474–4478.
[74] B. G. Dzikovski, V. A. Livshits, D. Marsh, *Biophys. J.* **2003**, *85*, 1005–1012.
[75] S. A. Simon, J. Gutknecht, *Biochim. Biophys. Acta Biomembr.* **1980**, *596*, 352–358.
[76] Y. N. Antonenko, P. Pohl, G. A. Denisov, *Biophys. J.* **1997**, *72*, 2187–2195.
[77] V. S. Sokolov, P. Pohl, *Biophys. J.* **2009**, *96*, 77–85.
[78] P. E. G. Thorén, D. Persson, M. Karlsson, B. Norden, *FEBS Lett.* **2000**, *482*, 265–268.
[79] G. Ter-Avetisyan, G. Tunnemann, D. Nowak, M. Nitschke, A. Herrmann, M. Drab, M. C. Cardoso, *J. Biol. Chem.* **2009**, *284*, 3370–3378.
[80] A. C. Chakrabarti, D. W. Deamer, *J. Mol. Evol.* **1994**, *39*, 1–5.
[81] E. Barany-Wallje, S. Keller, S. Serowy, S. Geibel, P. Pohl, M. Bienert, M. Dathe, *Biophys. J.* **2005**, *89*, 2513–2521.

Received: April 7, 2009
Published online on June 9, 2009

